

Potential Impacts of Climate Change on Flood-Induced Travel Disruptions: A Case Study of Portland, Oregon, USA

Heejun Chang,* Martin Lafrenz,* Il-Won Jung,* Miguel Figliozzi,† Deena Platman,‡ and Cindy Pederson‡

*Department of Geography, Portland State University

†Department of Civil and Environmental Engineering, Portland State University

‡Metro, Portland, Oregon

This study investigated potential impacts of climate change on travel disruption resulting from road closures in two urban watersheds in the Portland, Oregon, metropolitan area. We used ensemble climate change scenarios, a hydrologic model, a stream channel survey, a hydraulic model, and a travel forecast model to develop an integrated impact assessment method. High-resolution climate change scenarios are based on the combinations of two emission scenarios and eight general circulation models. The Precipitation-Runoff Modeling System was calibrated and validated for the historical period of 1988 and 2006 and simulated for determining the probability of floods for 2020 through 2049. We surveyed stream cross-sections at five road crossings for stream channel geometry and determined flood water surface elevations using the HEC-RAS model. Four of the surveyed bridges and roadways were lower in elevation than the current 100-year flood water surface elevation, leading to relatively frequent nuisance flooding. These roadway flooding events will become more frequent under some climate change scenarios in the future, but climate change impacts will depend on local geomorphic conditions. Whereas vehicle miles traveled was not significantly affected by road closure, vehicle hours delay demonstrated a greater impact from road closures, increasing by 10 percent in the Fanno Creek area. Our research demonstrated the usefulness of the integration of top-down and bottom-up approaches in climate change impact assessment and the need for spatially explicit modeling and participatory planning in flood management and transportation planning under increasing climate uncertainty. *Key Words:* climate change, integrated impact assessment, transportation, urban flooding.

According to the most recent Intergovernmental Panel on Climate Change report (IPCC 2007), anthropogenic climate change is projected to bring more frequent, heavier winter precipitation and earlier snowmelt in midlatitude areas. This is due to the fact that warmer air can hold more water vapor, thus accelerating the circulation of water between the atmosphere and land and oceans (Huntington 2006). As a result of rising intense precipitation and soil moisture content, water tables are likely to increase, leading to more frequent flooding in areas already affected by periodic flooding. This is evidenced by the recent flood events in 2006, 2007, and 2008 in the U.S. Pacific Northwest that severely limited surface transportation and thus disrupted the regional economy. Although there is ample need to investigate the vulnerability of regional transportation infrastructure and associated disruption of the transportation systems, very few studies have investigated the potential impacts or adaptation of climate change on the transportation sector (National Research Council [NRC] 2008; Koetse and Rietveld 2009) other than focusing on reducing green-

house gas emissions (Black and Sato 2007; Chapman 2007).

Of all the possible climate impacts on transportation, the greatest in terms of cost is that of urban flooding (IPCC 2007). In the last ten years, there have been four cases when flooding of urban underground rail systems has caused damage worth more than (10 million and numerous cases of lesser damage (Compton, Ermolieva, and Linnerooth-Bayer 2002). The 1996 flood in the Boston metropolitan area caused \$70 million in property damage, also disrupting business and personal travel. In the New York metropolitan area, torrential rainfall events in 2004 and 2007 sent water into the subway tunnels as the drainage system could not handle the excessive rainfall (Chan 2007).

To date, only a few studies have examined potential impacts or adaptation of climate change on transportation systems. These studies include regional economic impacts as a result of changing transportation modes in northern Canada (Lonergan, Difrancesco, and Woo 1993), and flood risk mapping for vulnerable roads and the cost of travel disruption in the Boston metropolitan

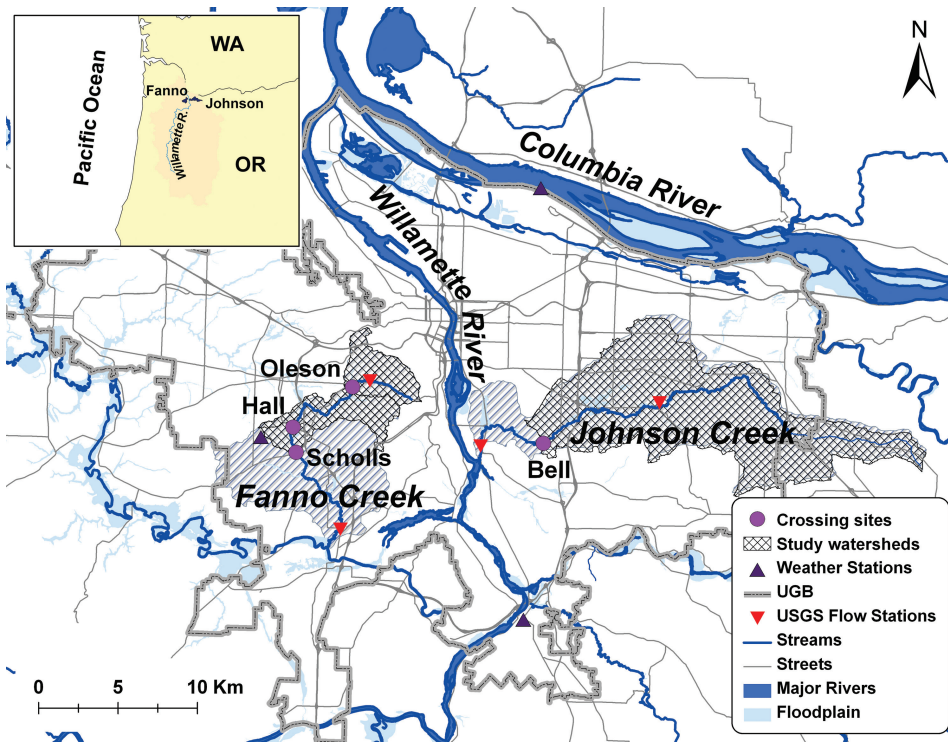


Figure 1. A map of the Portland metropolitan area and study watersheds. UGB = Xxxxxxx xxxxxxx Q2 xxxxxxx.

area (Suarez et al. 2005), in the New York metropolitan area (Jacob, Gornitz, and Rosenzweig 2007), in Maryland (Sohn 2006), and more comprehensively along the East Coast of the United States (ICF International 2008). These studies, however, used either synthetic climate change scenarios (e.g., hypothetical sea level rise) or a couple of climate change scenarios that offered only limited climate impact assessment and quantification of associated uncertainties (Wurbs, Toneatti, and Sherwin 2001). Furthermore, they did not model hydrology and geomorphology explicitly at specific intersections of streams and roads, which can vary significantly at a local scale. Only recently have researchers started to investigate potential adaptation of railways in Sweden (Lindgreen, Jonsson, and Carlsson-Kanyama 2009) and in the United Kingdom (Dobney et al. 2009).

Studies on natural hazard impacts from future climate change have struggled to adequately assess impacts (Soleckie and Rosenzweig 2001). This is largely due to a lack of adequate data, difficulty in interpreting the existing multidisciplinary data, the complexity of cascading effects resulting from flooding on the regional transportation systems (NRC 1999), and the focus on attempting to model only extreme events, which are inherently more difficult to predict and model (Pielke and Downton 2000; Changnon 2003). With this study, a multidisciplinary team of scientists and urban plan-

ners focus on the cumulative effects of a range of flood events, which are likely to increase in frequency as a result of climate change. In addition, we model the short-term transportation impact from temporary flooding in a few local roadways.

Study Area

Two creeks—Johnson Creek and Fanno Creek—in the Portland metropolitan area serve as our study sites (Figure 1). These two creeks were chosen because they have historical flow data and exhibit high flooding potential; each also has high road density (Table 1). Daily vehicle miles of travel in Portland increased from 19.4 million to 29.2 million between 1990 and 2007 (Metro 2009). With different slopes and different degrees of urban development, the hydrological processes of the two watersheds are different (Fanno—highly urbanized and steep slopes; Johnson Creek—mixed land use with gentle slopes); each serves as a representative for other urban watersheds. Both streams are part of the Lower Willamette River watershed. The 42-km Johnson Creek stems from west of the Cascade Range and flows into the Willamette River just north of Elk Rock Island, whereas the 24-km Fanno Creek originates within the Portland city limits and drains into the Tualatin River at river mile 9.3.

Table 1. Characteristics of each crossing basin

| Subbasin | Area (km ²) | Mean elevation (m) | Mean slope (degrees) | Road density (km/km ²) | Land use (%) | | | | |
|----------|-------------------------|--------------------|----------------------|------------------------------------|--------------|-------|--------|--------------|---------|
| | | | | | Urban | Water | Forest | Agricultural | Wetland |
| Oleson | 12.8 | 158 | 7.75 | 12,399 | 78.30 | 0.00 | 21.61 | 0.08 | 0.00 |
| Hall | 26.7 | 125 | 5.75 | 11,927 | 83.58 | 0.00 | 15.60 | 0.16 | 0.66 |
| Scholls | 30.6 | 118 | 5.31 | 11,763 | 84.56 | 0.02 | 13.59 | 1.10 | 0.73 |
| Bell | 117.6 | 134 | 4.57 | 7,726 | 59.41 | 0.04 | 18.70 | 20.92 | 0.92 |

Largely belonging to the marine West Coast climate, the study area exhibits wet, mild winters and dry, warm summers with annual precipitation amounts ranging from 1,000 mm at the mouth of both creeks to 1,500 mm in the headwaters. Precipitation variability is influenced by three- to five-year cycles of ENSO events and the twenty- to thirty-year cycle of alternating phases of the Pacific Decadal Oscillation. Located at a relatively low altitude, snowmelt is not a big component of the hydrologic cycle in either watershed. Accordingly, streamflow is typically highest during winter months when flooding potentials are high (December to February). Both streams' discharge patterns exhibit the typical behavior of urban streams in the Pacific Northwest, with flashy and relatively high flow during winter rainfall periods and low flows dominated by groundwater discharge during the dry summer (Chang 2007).

Soil characteristics of the two watersheds are closely associated with bedrock lithology and elevation. The upper portion of Fanno Creek has moderately deep, somewhat poorly drained silt loam soils and significant areas of urban land dominated by impervious surfaces (Green 1983); the lower portion of the watershed includes deep, somewhat poorly drained and moderately well-drained silt loams (Green 1982). The upstream areas of Johnson Creek have moderately deep and somewhat poorly drained silt loams, and lower Johnson Creek has more urban land and very deep, well-drained silt and gravelly loam soils (Gerig 1985). Soil permeability in both creeks reflects elevation gradients.

For all basins, urban land use is the dominant use, including more than 50 percent of each basin. In Fanno Creek, urban land use is increasing in downstream basins at the expense of forested areas. Because the upper portion of Johnson Creek is outside of the urban growth boundary, this basin contains a relatively high proportion of agricultural lands. However, a portion of Upper Johnson Creek was incorporated into the urban growth boundary in 2002.

Data and Methods

Integrated Impact Assessment

Figure 2 exhibits the methodological framework of the integrated assessment of climate change on urban flooding and transportation systems. This framework combines a traditional top-down impact assessment approach with a bottom-up vulnerability analysis. Developing climate change scenarios and downscaling for hydrologic impact assessment follow a traditional top-down approach. Regional stakeholders—the county transportation planner, the regional transportation group, local watershed councils, and community volunteers—were involved at the beginning of the project, informing researchers on the history of flooding and identifying vulnerable transportation nodes. They also provided feedback on our research throughout the project period. Although assessments of climate change impacts, adaptation, and vulnerability become sophisticated (Carter et al. 2007), particularly at the regional scale (Knight and Jäger 2009), to our knowledge, this is the first attempt to apply an integrated assessment approach in the transportation sector.

Climate Scenarios

We used two different sets of climate data for climate modeling. First, observed daily precipitation and temperature from the PDX airport and Beaverton stations (Oregon Climate Service 2008) were used for hydrologic modeling. Second, statistically down-scaled climate change data at a spatial resolution of 1/16 degree (Salathé, Mote, and Wiley 2007) from sixteen different climate simulations were used for climate impact assessment. We used the combinations of eight coupled atmosphere ocean global climate models and two greenhouse gas emission scenarios to explore uncertainty associated with global climate model (GCM) structure and greenhouse gas emission

Table 2. Description of global climate models used in this study (Randall et al., 2007)

| Model ID | Acronym | Country | Spatial resolution | | Reference |
|---------------------|---------|----------------|--------------------|---------------|--------------------------|
| | | | Atmosphere | Ocean | |
| CCSM3 | CCSM3 | United States | 1.4° × 1.4° | 1.0° × 1.0° | Collins et al. (2006) |
| CNRM-CM3 | CNRM | France | 1.9° × 1.9° | 2.0° × 2.0° | Terray et al. (1998) |
| ECHAM5/MPI-OM | ECHAM5 | Germany | 1.9° × 1.9° | 1.5° × 1.5° | Jungclaus et al. (2005) |
| ECHO-G | ECHO-G | Germany/Korea | 3.9° × 3.9° | 2.8° × 2.8° | Min et al. (2005) |
| IPSL-CM4 | IPSL | France | 2.5° × 3.75° | 2.0° × 2.0° | Marti et al. (2005) |
| MIROC3.2 (high res) | MIROC | Japan | 1.1° × 1.1° | 0.2° × 0.3° | K-1 Developers (2004) |
| PCM | PCM | United States | 2.8° × 2.8° | 0.7° × 1.1° | Washington et al. (2000) |
| UKMO-HadCM3 | UKMO | United Kingdom | 2.5° × 3.75° | 1.25° × 1.25° | Gordon et al. (2000) |

scenarios (Cameron 2006; see also Table 2). The years between 1970 and 1999 serve as a reference period, and the years between 2020 and 2049 serve as a future period representing the years around 2035.

The simulated precipitation and temperature data from the downscaled scenarios were compared with observed weather station data. When there were substantial biases in the downscaled data, these biases were

corrected using quantile mapping (Wood et al. 2004). The bias-corrected data were then used as input to the hydrologic simulation model. Figure 3 shows changes in monthly precipitation and temperature for the study area. As shown in Figure 3, January and February precipitation amounts are generally projected to increase, whereas July precipitation is projected to decline regardless of emission scenarios. Temperature is projected to

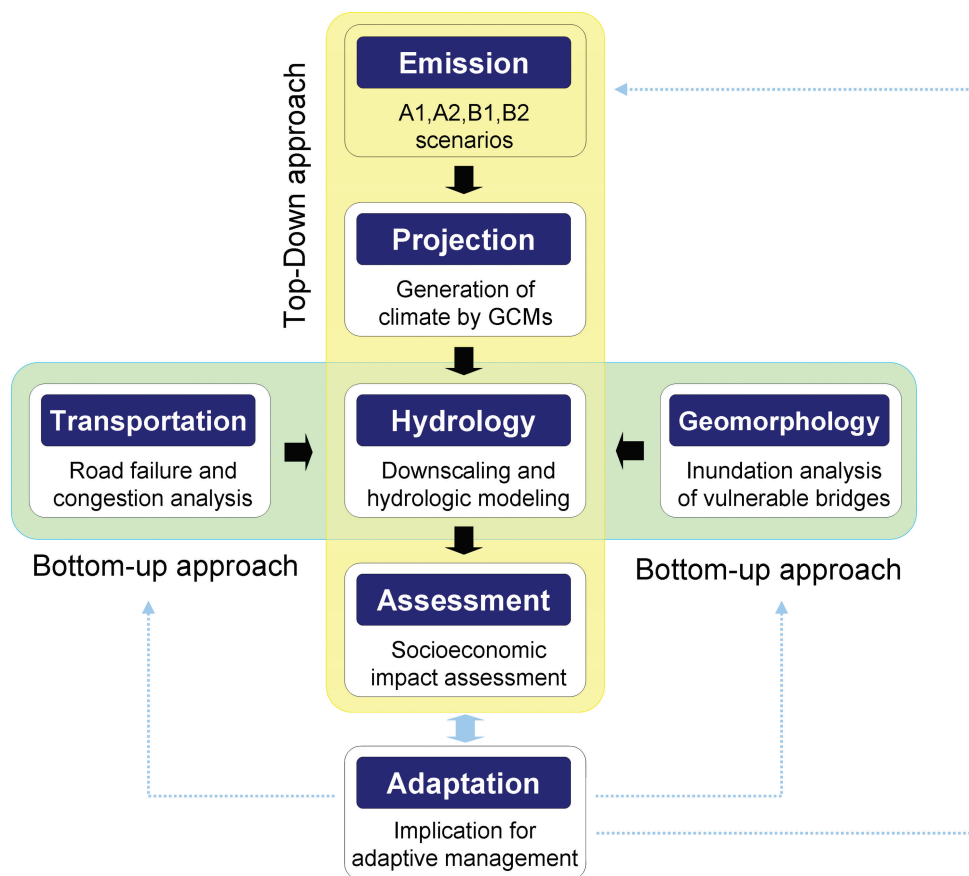


Figure 2. An integrated assessment of climate change impacts on transportation system. The dotted arrows indicate feedbacks not modeled in this study. GCMs = global climate models.

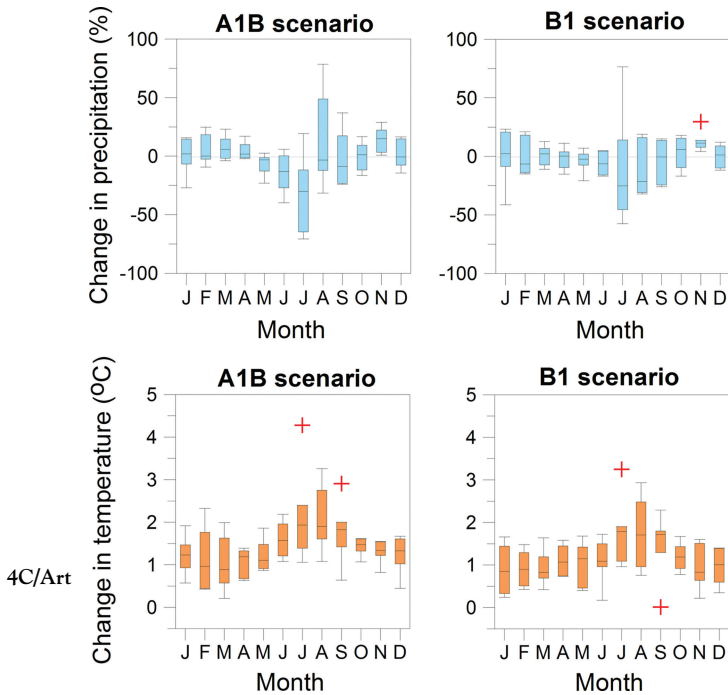


Figure 3. Changes in future (2020–2049) monthly precipitation and temperature from the reference period (1970–1999) under sixteen climate change scenarios (eight for A1B, eight for B1) for the Portland metropolitan areas. + indicates outliers that fall outside of whisker lengths.

210 increase overall with higher increases under the A1B emissions scenario.

Hydrologic Modeling

215 The U.S. Geological Survey (USGS) Precipitation Runoff Modeling System (PRMS) model simulates runoff changes and resulting changes in flood frequency. This model has been used in climate impact assessment for a range of watersheds around the world (Burlando and Rosso 2002; Dagnachew, Christine, and Francoise 2003; Bae, Jung, and Chang 2008). PRMS uses observed daily mean precipitation and maximum and minimum temperature to simulate daily streamflow. PRMS is a semidistributed, physically based watershed model, based on hydrologic response units (HRUs; Leavesley et al. 2002), which is ideal for simulating changes in flow under different environmental scenarios, including climate change. HRUs, assumed to be homogeneous with respect to hydrologic response to climate condition, are partitioned by using a combination of slope, aspect, land use, soil type, and geology.

220
225
230 PRMS model parameters are calibrated focusing on sensitive parameters, which are based on the literature (Laenen and Risley 1997). Some parameters are di-

235 rectly estimated from the measurable basin characteristics in geographic information system (GIS) layers (see Table 3). The remaining parameters (shaded in Table 3) are estimated by Rosenbrock’s (1960) automatic optimization method. PRMS is calibrated and verified for the four gauged sites for the period between 1988 and 2006 (see Table 4). The widely used Nash and Sutcliffe nondimensional model efficiency criterion was used to evaluate the performance of PRMS. The values in excess of 0.6 indicated a satisfactory fit between observed and simulated hydrographs (Wilby and Harris 2006). We applied the calibrated model for the ungauged cross-section survey sites using the regionalization method (Wagener and Wheater 2006).

245 Additionally, we used the Web-based GIS application StreamStats, which was developed by the USGS (<http://water.usgs.gov/osw/streamstats/index.html>), to determine the two-year, five-year, ten-year, twenty-five-year, fifty-year, and hundred-year discharge values for each of the five surveyed crossing locations. StreamStats uses a regional regression analysis to calculate the discharge for subbasins and an area to discharge relationship to determine the discharge to a user-selected location on a stream. The regression equations are specific to a particular region; our study areas fall completely within Oregon flood region 2b, which includes all basins between the crests of the Cascade and Coast Ranges with a mean basin elevation of less than 3,000 feet (Cooper 2005).

Channel Survey and Hydraulic Analysis

265 To evaluate future flooding impacts at actual road crossings identified by stakeholders, we conducted stream channel surveys at five different road crossings and conducted a hydraulic analysis with HEC-RAS, which has been used to find water surface elevations for historical floods (Benito, Diez-Herrero, and de Villalta 2003) and to model water flowing through bridges and culverts (Hotchkiss et al. 2008). With this approach, we determined the discharge value necessary to produce roadway flooding at each road crossing. We surveyed and modeled road flooding at five different bridge sites. There are three sites on Fanno Creek—Oleson Road, upstream Hall Boulevard, and the downstream Scholls Ferry Road crossing—and two sites on Johnson Creek—the Bell Avenue and Linwood Avenue crossings. Based on daily vehicle miles traveled, each road is classified as either an arterial or major arterial and, except for Oleson Road, also serves as a bus line. Four of the five locations have a history of road flooding during

Table 3. Precipitation Runoff Modeling System model parameters used for calibration

| Parameter | Description | Range | Initial values | Calibrated values | Source |
|--------------------|--|---------------|----------------|-------------------|--------|
| hru_elev | Mean elevation for each HRU, in feet | -300-30,000 | — | 117-602 | D |
| hru_slope | HRU slope in decimal vertical feet/horizontal feet | 0-10 | — | 0.01-0.09 | D |
| cov_type | Cover type (0 = bare, 1 = grasses, 2 = shrubs, 3 = trees) | 0-1 | — | 0-3 | L |
| covden_sum | Summer vegetation cover density | 0-1 | — | 0.01-0.9 | L |
| covden_win | Winter vegetation cover density | 0-1 | — | 0.01-0.8 | L |
| wrain_intcp | Winter rain interception storage capacity, in inches | 0-5 | — | 0.001-0.05 | L |
| srain_intcp | Summer rain interception storage capacity, in inches | 0-5 | — | 0.001-0.05 | L |
| snow_intcp | Winter snow interception storage capacity, in inches | 0-5 | — | 0.001-0.1 | L |
| hru_percent_imperv | HRU impervious area, in decimal percent | 0-1 | — | 0.1-0.6 | L |
| soil_type | HRU soil type (1 = sand, 2 = loam, 3 = clay) | 1-3 | — | 1-3 | S |
| soil_moist_max | Maximum available water holding capacity in soil profile, in inches | 0-20 | — | 5-9 | S |
| soil_rechr_max | Maximum available water holding capacity for soil recharge zone, in inches | 0-10 | — | 1-2 | S |
| hamon_coef | Hamon evapotranspiration coefficient | 0.004-0.008 | 0.0055 | 0.004-0.008 | R |
| soil2gw_max | Maximum rate of soil water excess moving to ground water | 0.0-5.0 | 0.15 | 0.12-0.15 | R |
| smidx_coef | Coefficient in nonlinear surface runoff contributing area algorithm | 0.0001-1.0000 | 0.01 | 0.001 | R |
| smidx_exp | Exponent in nonlinear surface runoff contribution area algorithm | 0.2-0.8 | 0.3 | 0.20-0.21 | R |
| ssrcoef_sq | Coefficient to route subsurface storage to streamflow | 0.0-1.0 | 0.1 | 0.05-0.44 | R |
| ssrcoef_lin | Coefficient to route subsurface storage to streamflow | 0.0-1.0 | 0.1 | 0.0001 | R |
| ssr2gw_exp | Coefficient to route water from subsurface to groundwater | 0.0-3.0 | 1.0 | 0.5-3.0 | R |
| ssr2gw_rate | Coefficient to route water from subsurface to groundwater | 0.0-1.0 | 0.1 | 0.006-0.02 | R |
| gwflow_coef | Groundwater routing coefficient | 0.000-1.000 | 0.015 | 0.003-0.07 | R |

Note: HRU = hydrological response unit; D = digital elevation map (10 m resolution); L = land use map; S = soil map; R = Rosenbrock method.

large storm events (Oregonian 2007). The Scholls Ferry Road bridge is a relatively large span with no history of flooding; this site was selected as a probable example of a correctly sized structure with respect to climate-

change-induced flooding. All sites are located between USGS gauging stations.

We collected the channel geometry data by following stream channel reference site protocol for

Table 4. Precipitation Runoff Modeling System model performance for calibration and verification period

| Catchment (area, km ²) | Calibration period (Verification period) | <i>r</i> | RMSE | NSE |
|------------------------------------|--|-------------|-------------|-------------|
| Upper Fanno (6.1) | 2001-2003 (2003-2006) | 0.84 (0.86) | 1.31 (1.26) | 0.69 (0.74) |
| Lower Fanno (80.5) | 2001-2003 (2003-2006) | 0.87 (0.80) | 1.26 (1.67) | 0.74 (0.62) |
| Upper Johnson (68.3) | 1988-1998 (1999-2006) | 0.82 (0.85) | 1.73 (1.56) | 0.66 (0.65) |
| Lower Johnson (132.1) | 1988-1998 (1999-2006) | 0.83 (0.81) | 1.35 (1.17) | 0.64 (0.62) |

Note: RMSE = Root mean square error = $\sqrt{\sum (O_i - S_i)^2/n}$, where *n* is a number of data; *r* = correlation coefficient (R) = $SS_{os}/\sqrt{SS_o \times SS_s}$, $SS_{os} = \sum (O_i - \bar{O})(S_i - \bar{S})$, $SS_o = \sum (O_i - \bar{O})^2$, $SS_s = \sum (S_i - \bar{S})^2$ where *O* is observed flow and *S* is simulated flow; NSE = Nash-Sutcliffe efficiency = $1 - \frac{\sum (O_i - \bar{O})^2 - \sum (O_i - S_i)^2}{\sum (O_i - \bar{O})^2}$, where \bar{O} is mean observed flow.

290 wadeable streams (Harrelson, Rawlins, and Potyondy
1994). We surveyed four cross-sections at each site
with two upstream and two downstream of the bridge
and captured the bridge geometry relative to the cross-
sections. At each cross-section we noted the elevation
295 at the top of the banks and the water surface elevation;
all cross-sections and bridge information were tied to
a common datum to model water flowing through the
reach. Using a flow meter, we measured stream velocity
300 at the furthest upstream cross-section and, for the pur-
pose of calibrating the models, estimated the roughness
(Manning's n) at each cross-section (Chow 1959). In
HEC-RAS we conducted a combined steady flow analysis
using the bridge routine calibrated to our known
water surface elevations for each cross-section.

305 Transportation Impacts Methodology

To measure the potential disruption and costs of
flooding on the transportation system, we used the
Metropolitan Planning Organization's (MPO) four-step
model and multimodal equilibrium traffic assignment
procedures. The model produces current (2005) and fu-
310 ture (2035) travel volumes based on growth, land use,
and transportation assumptions in each time period.
Household and employment estimates are assigned to a
transportation analysis zone (TAZ), the "unit geogra-
315 phy" for travel within the demand model. All the trips
generated by the land use elements are aggregated and
analyzed at the TAZ level. The travel model estimates
the number of trips that will be made, the distribution
patterns of the trips throughout the region, the likely
320 mode used for the trip, and the actual roadways and
transit lines used for auto, truck, and transit trips. Trip
assignment applies the Frank-Wolfe algorithm (1956)
to determine equilibrium flows in the transportation
network. Trip paths are assigned between origins and
325 destinations based on capacity, volume, and speed; trips
will take the shortest and quickest path. Disruption on
the path, such as flooding, will redistribute flows to other
routes.

We acknowledge that the MPO's four-step travel
330 forecast model provides a coarser level of output than
is ideal for this type of research. Advance assignment
methods such as dynamic traffic assignment (DTA)
and microsimulation exist that more effectively capture
traffic flow diurnal characteristics, the effects of queu-
335 ing, and the duration of congestion that might result
from a flooding event (Mahmassani 2001; Peeta and
Ziliaskopoulos 2001). However, for the purpose of the
study, we assumed that flooding events are forecasted

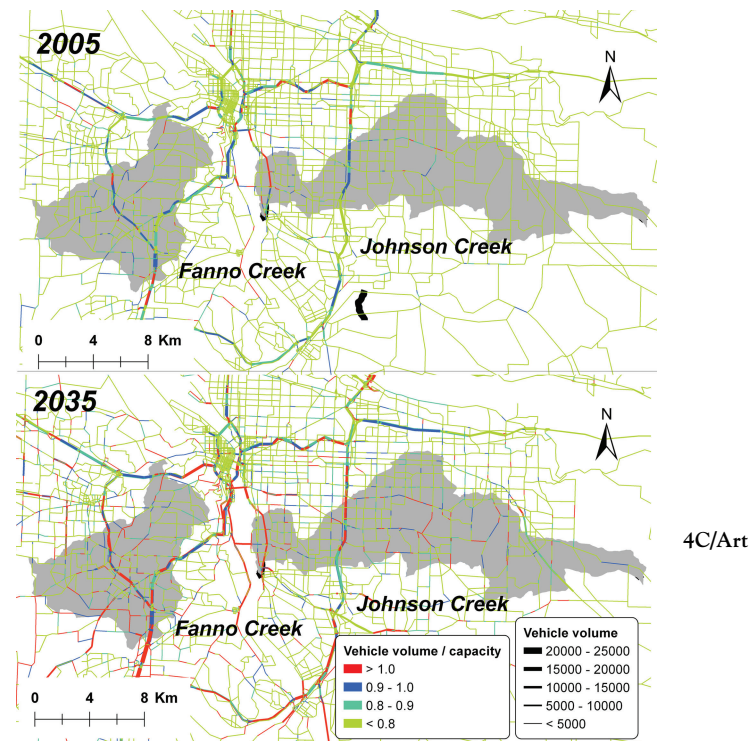


Figure 4. Changes in auto traffic volumes in the study area for 2005 and 2035.

and drivers have full information regarding the closure
of the road crossings. Metro, the MPO, is currently de- 340
veloping DTA capabilities for use in exactly this type
of application. These methods are more fully described
in the NRC (2007) report.

The traffic analysis began with the identification of
transportation network links that are expected to flood 345
based on the findings from the climate and hydrologi-
cal analysis. It is important to note that the analysis
focused on route diversion only and did not alter origin-
destination pattern. Initial one-hour midday and two-
hour afternoon peak traffic assignments were run using 350
Equilibre Multimodal/Multimodal Equilibrium software
to establish baseline traffic volumes and link volume
and capacity for 2005 and 2035 (Figure 4). Traffic as-
355 signments were then rerun with the flooded network
links removed for both the Fanno Creek and Johnson
Creek study areas. Using this output, a flood area of
influence, comprised of TAZ clusters, was identified for
each study area. Transportation evaluation measures
were produced for each flood area of influence that in-
360 cluded vehicle miles traveled, vehicle hours, and vehi-
cle hours of delay for the one-hour midday and two-hour
afternoon peak travel periods.

Results and Discussion

Changes in Flood Frequency

365 We estimated the changes in flood frequency with
 different recurrence intervals by using the PeakFQ
 program developed by the USGS (Flynn, Kirby, and
 Hummel 2006). The PeakFQ provides estimates of in-
 370 stantaneous annual-maximum peak flows with recur-
 recurrence intervals of two, five, ten, twenty-five, fifty, and
 one hundred years based on flood-frequency analyses
 recommended in Bulletin 17B (Interagency Advisory
 Committee on Water Data 1982). With this method,
 we constructed annual peak flows using simulated daily
 375 discharge values by the PRMS model for 1970 through
 1999 and for 2020 through 2049 at the four study areas.

Recurrence flood flows for the reference period
 demonstrate that the simulated results by the PRMS

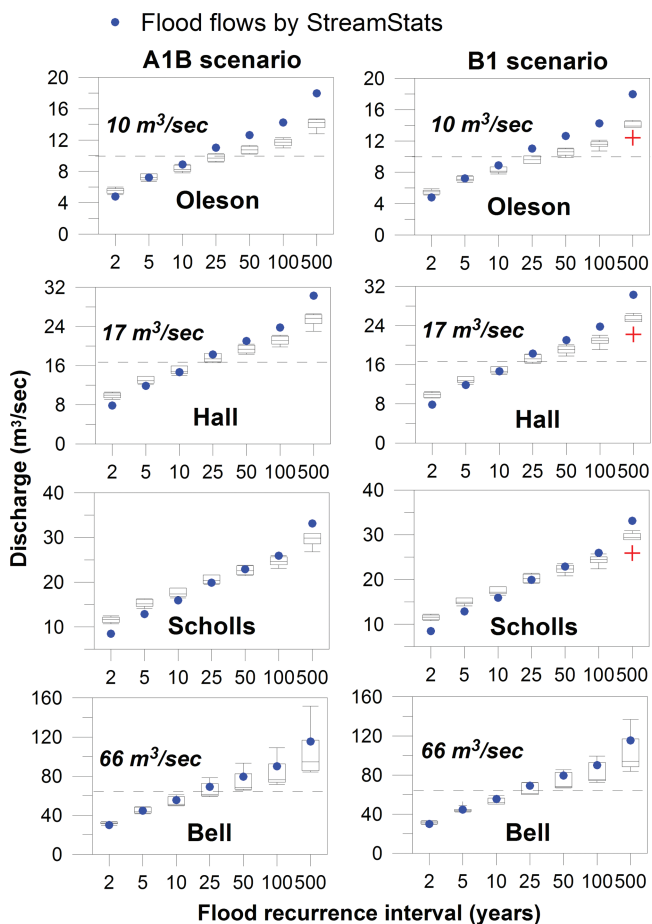


Figure 5. Comparison of estimated flood flows by USGS StreamStats and simulated flood flows by the Precipitation Runoff Modeling System model using sixteen climate change scenarios (eight for A1B, eight for B1) for each subbasin from 1970 to 1999. + indicates outliers that fall outside of whisker lengths.

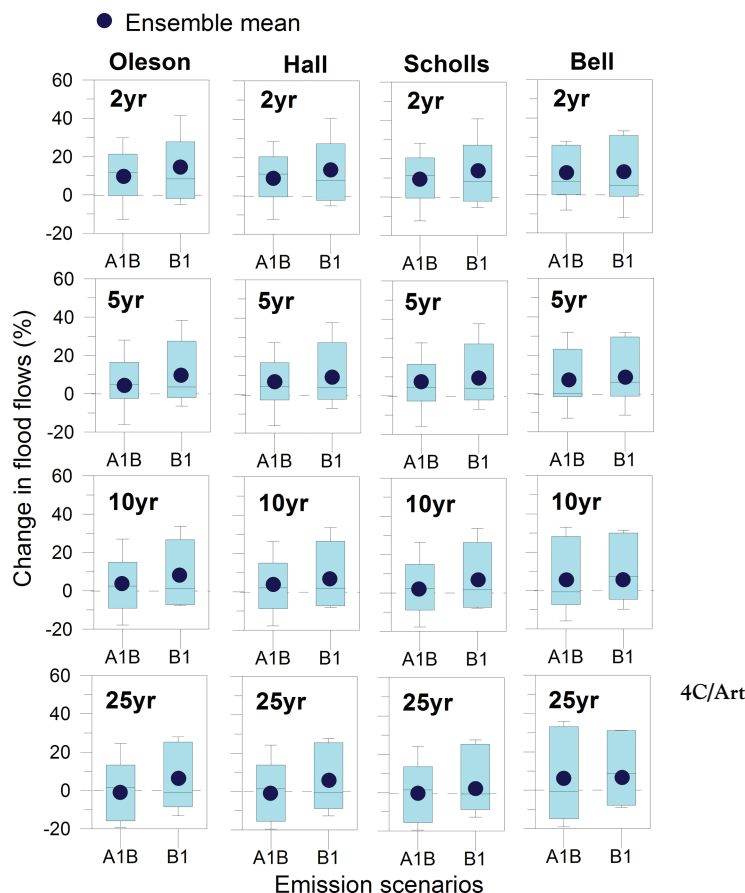


Figure 6. Changes in flood flows with recurrence flood intervals for two, five, ten, and twenty-five years under A1B and B1 scenarios.

using the downscaled climate simulations agree well
 with estimated flood flows from the USGS StreamStats 380
 (Figure 5). In particular, the below twenty-five-year re-
 currence flood flows more closely match with the USGS
 StreamStats results. Most inundated flood flows (dashed
 lines) occur between the ten-year and twenty-five-year
 385 recurrence flood flows except at the Scholls Ferry site.
 The over fifty-year recurrence flood flows are highly af-
 fected by the different GCM structures; however, the
 emission scenario impacts reveal relatively fewer differ-
 ences than the GCM structure.

The recurrence flood flows for 2020 through 2049 390
 represent the differences in the direction of change
 according to recurrence interval and the GCM
 simulations. As shown in Figure 6, ensemble averaged
 two-year, five-year, and ten-year recurrence flood flows
 395 at all sites increase, whereas the ensemble mean
 flood flows for twenty-five-year recurrence interval does not
 change under the A1B scenario. They do, however,
 increase under some climate change scenarios, suggest-

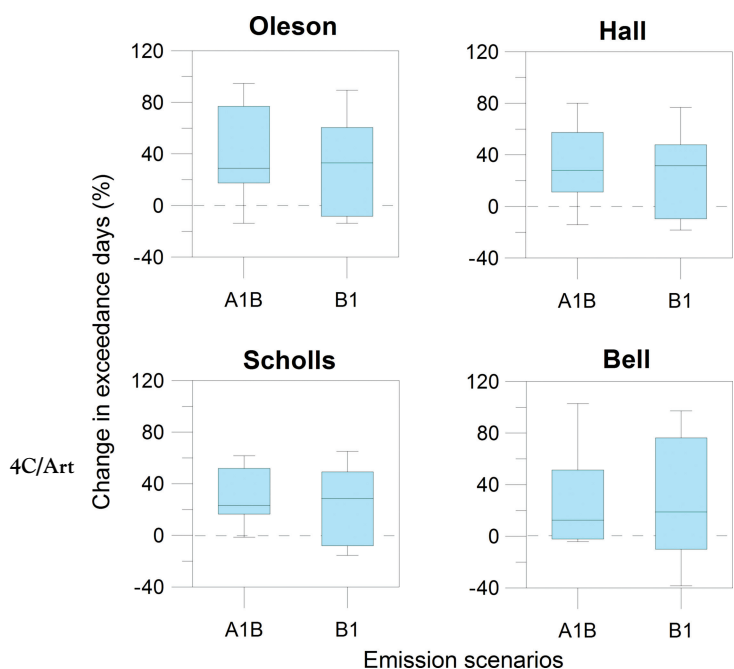


Figure 7. Changes in exceedance days with total days exceeding two-year recurrence flood interval for each subbasin.

ing that the magnitude and directions of change in the higher flood flows in the study areas are more affected by GCM structures than the emission scenarios.

Figure 7 shows the change in days that exceeded the two-year recurrence flood flows. These values show approximately thirty to sixty days for the reference period and thirty to eighty days for 2020 through 2049. Although the mean of the exceedance days increases at all sites, the GCMs and the emission scenarios remain as the main source of uncertainty, with higher uncertainty associated with the choice of GCM. Our finding is consistent with other previous studies. For example, the largest source of uncertainty was the GCM structure in U.K. catchments (Wilby and Harris 2006; Kay et al. 2009). Exceedance probability of the inundated discharge for ensemble mean does not change remarkably (Table 5). However, the differences between high and low scenarios remain high, indicating that the quantification of uncertainty resulting from climate impact assessment is key in supporting new transportation system design.

Changes in the Probability of Road Flooding

The HEC-RAS model output shows that all cross-sections with the exception of Scholls Ferry Road are inundated during the current twenty-five-year flood event (Figure 8). However, the crossings diverge somewhat for

Table 5. Exceedance probability of the threshold flood discharge under high, ensemble mean, and low climate change scenarios

| Climate scenarios | Oleson | | Hall | | Bell | |
|-------------------|--------|--------|-------|--------|-------|--------|
| | Ref | Future | Ref | Future | Ref | Future |
| A1B | | | | | | |
| High | 0.050 | 0.100 | 0.070 | 0.120 | 0.080 | 0.120 |
| Mean | 0.041 | 0.041 | 0.051 | 0.050 | 0.042 | 0.050 |
| Low | 0.025 | 0.002 | 0.035 | 0.005 | 0.020 | 0.002 |
| B1 | | | | | | |
| High | 0.050 | 0.130 | 0.060 | 0.180 | 0.070 | 0.100 |
| Mean | 0.040 | 0.038 | 0.050 | 0.060 | 0.042 | 0.051 |
| Low | 0.018 | 0.002 | 0.030 | 0.010 | 0.025 | 0.017 |

smaller events. The Oleson Road crossing floods much more frequently; this crossing area has an active floodplain upstream of the bridge but is controlled downstream by a wooden wall and riprap. This crossing is well known as a problem flood area, and our modeling simply reinforces the frequency with which this bridge can become impassable due to flooding. The Hall Boulevard crossing is flooded during less than a twenty-five-year magnitude event; this crossing has a much more extensive floodplain than the Oleson Road crossing and the channel is not constricted other than when passing

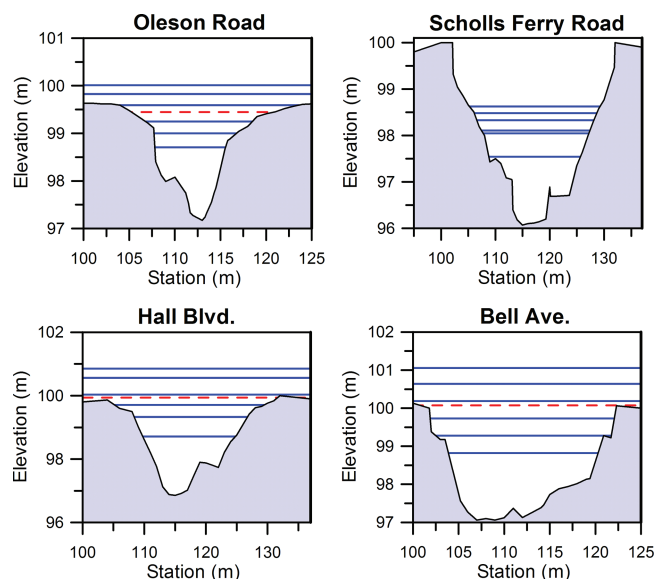


Figure 8. Stream channel cross-sections with solid horizontal lines indicating the water surface elevations for, from bottom to top, the two-year, five-year, ten-year, twenty-five-year, fifty-year, and hundred-year events. The dashed line indicates the water surface elevation when water first begins flooding the road; this never occurs at Scholls Ferry Road. Linwood Avenue is nearly identical to Bell Avenue, so the stream channel cross-section is not reported here.

through the bridge. Yet, the bridge opening itself is not large; hence, this road is subject to fairly frequent flooding. This bridge is crowned, as is Scholls Ferry Road, and the stream does not cover the bridge during any flood event; however, water does flow across the road in the floodplain during high water, which leads to closure of this crossing. With a large floodplain and a large bridge opening, the Scholls Ferry Road crossing does not flood at any discharge; however, the bike path adjacent to the stream that goes under the bridge is often inundated.

The bridge openings in Johnson Creek are much larger than most bridge openings in Fanno Creek, a legacy of channelization in Johnson Creek. Yet, each crossing site floods just prior to a twenty-five-year event. Like the Hall Boulevard site, these roadways begin flooding before water overtops the bridge itself. In the case of the Bell Avenue crossing, water will actually flow north of the stream channel, through a parking lot, and across the road approximately 3 m north of the bridge itself; hence, this road is closed more frequently than would be expected by our models.

Our results show that although floods depend on precipitation intensity, volume, and timing, they also rely on drainage basin and local geomorphic characteristics. However, given the predicted increases in flood return exceedance for smaller floods (Figure 6), nuisance flooding is likely to become more common at these cross-sections. As illustrated in this study, restoration of floodplains will serve as a proactive adaptation strategy in reducing flood damage under a changing climate. In addition, future flooding potential could be further reduced as best management practices such as porous pavement or detention ponds are implemented. In particular, older neighborhoods (e.g., lower Johnson Creek) would be good candidate areas for implementing these practices.

Impacts on Transportation Network

The Fanno Creek and Johnson Creek flood areas of influence generate an estimated 973,000 and 541,000 vehicle miles traveled (VMT), respectively, in the two-hour afternoon peak travel period. Together, these areas account for 24 percent of the total VMT generated in the 4:00 p.m. to 6:00 p.m. travel period. They are located in suburban locations where the arterial street network is fairly complete but the local street network is often discontinuous. Table 6 lists the street links prone to flooding and the average traffic volume they carry in the two-hour afternoon peak travel period for the base year 2005 and future year 2035.

Table 6. Changes in average traffic volume as a result of road closures for 2005 and 2035

| Facility | Two-hour afternoon peak | | | |
|-----------------------|-------------------------|----------|----------|----------|
| | 2005 | | 2035 | |
| SW Oleson Rd | 900 NB | 1,200 SB | 1,000 NB | 1,400 SB |
| SW Hall Blvd | 3,800 NB | 2,800 SB | 4,400 NB | 3,300 SB |
| SE Johnson Creek Blvd | 1,800 EB | 1,600 WB | 2,800 EB | 2,300WB |
| SE Bell St | 400 NB | 600 SB | 500 NB | 800 SB |
| SE Linwood St | 1,550 NB | 1,600 SB | 1,550 NB | 1,750 SB |

Note: NB = northbound travel; SB = southbound travel; EB = eastbound travel; WB = westbound travel.

An evaluation of the travel model output for the Fanno Creek and Johnson Creek flooding areas of influence forecasted negligible increases (less than 1 percent) in VMT in both travel periods for 2005 and 2035 when flooded links were removed from the street network (Figure 9). Vehicle hours delay (VHD) demonstrates a greater impact from flooding. Closing facilities in the Fanno Creek travel shed causes more than 200 additional hours of delay in the afternoon peak period. The base and future years show similar increases in hours, but the percentage increase is much higher for 2005. The Johnson Creek travel shed's increase ranges from 4 percent in the base year to 3.4 percent in the future. The impacts of closing these facilities due to flooding are minimal on overall miles traveled, but they do reveal that other roadways will be more congested, resulting in greater delays because the diverting vehicles and existing vehicles are all affected.

The region-wide modeled transportation network provides several alternative routes to the flooded links. The macrolevel equilibrium traffic assignment assumes that travelers have perfect knowledge of the road conditions (without any incidents) and know which additional routes are available in time to make an informed decision about the path they will take. Therefore, the resulting statistics might underestimate the level of out-of-direction travel that would contribute to an increase in VMT during a short-term flooding event. Our findings are similar to other studies that show that the cost of delays and lost trips would be relatively small compared with damage to the infrastructure and to other property (Suarez et al. 2005; Kirshen, Knee, and Ruth 2008). This is due to the relatively large number of transportation networks and trips, a typical characteristic in mature metropolitan area.

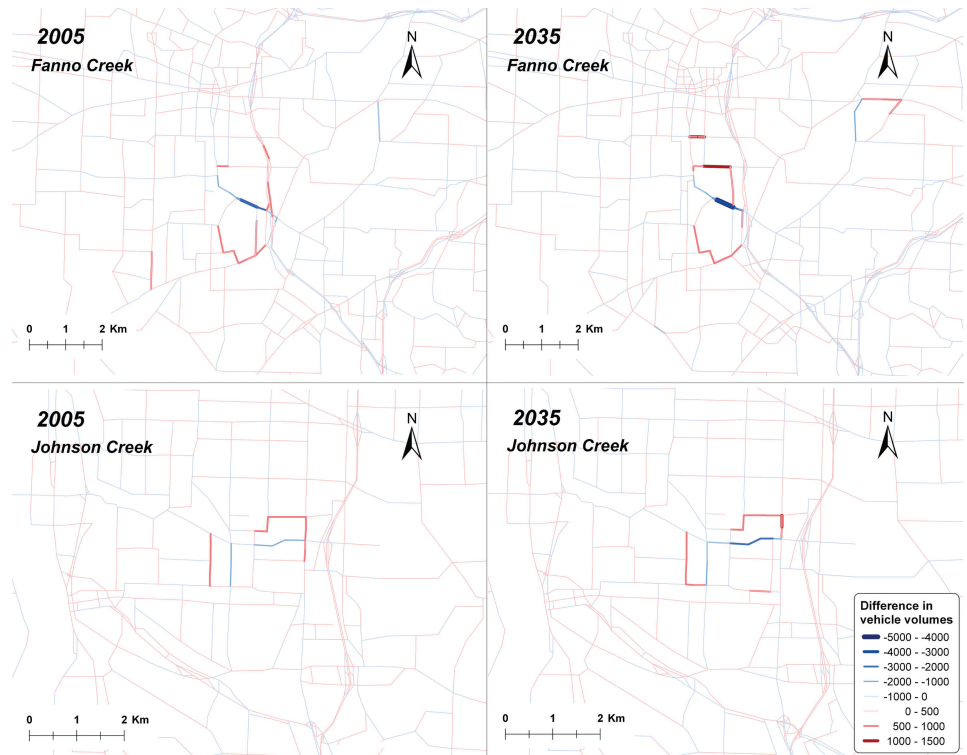


Figure 9. Changes in travel disruption as a result of road closure, 2005 and 2035 for Fanno Creek and Johnson Creek.

4C/Art

520 **Conclusions**

Global climate change will have significant impacts, particularly in urban areas where many socioeconomic activities are concentrated (Chang and Franczyk 2008). Many growing urban areas such as the U.S. Pacific Northwest will experience higher amounts and intensity of winter precipitation. In projecting future flood frequency, there are high uncertainties associated with GCM structure and emission scenarios. Despite this uncertainty, the five-year, ten-year, and other relatively small events are likely to increase in all study sites that have a history of chronic flooding. Stream channels will likely lag in adjusting to the new, slowly increasing discharge regimes and might not be able to adjust at bridge locations, which is likely to only further exacerbate roadway flooding. Although VMT in both periods show negligible increases, VHD demonstrated a greater impact from flooding. The estimates are, however, conservative, as the current approach assumes travelers' perfect knowledge regarding the closure of the road crossings.

Our results show that there is a nonlinear relation between precipitation change and urban flooding and that impacts on travel disruption are subject to local hydroclimate and geomorphic conditions. Although it is a specific case study, the integrated methodology used

in this study can be applied to other urban areas facing similar transportation impact in a changing climate. If climate change, watershed hydrology, channel morphology, and transportation networks are readily available in a spatial database, it could even be possible to upscale a similar model to regional or national levels. However, the complex interactions of a changing precipitation regime, adjustments in channel morphology, and human response and adaptation to flooding still need to be further investigated. Both natural and human systems coevolve over time with complex feedbacks at multiple spatial and temporal scales in response to external changes. Thus, further research should include continuous monitoring of the system and the development of coupled system dynamics models.

Despite some of these limitations, this study is one of the few interdisciplinary attempts to assess potential impacts of climate change on the transportation sector. The integration of the top-down and the bottom-up approaches involving local stakeholders at the beginning of the project demonstrates a useful tool to assess climate change impacts at a local scale. A participatory regional integrated assessment tool found in other sectors such as water resources and agriculture (e.g., Holman et al. 2008) could be adapted for the transportation sector. Such integrated knowledge and spatially explicit modeling is essential for establishing proactive flood and

transportation management planning and policies under increasing climate uncertainty.

575 Acknowledgments

This research was supported by the Oregon Transportation Research and Education Consortium (Grant number 2009–257). Additional support for Il-Won Jung was provided by the James F. and Marion L. Miller Foundation’s postdoctoral fellowship in sustainability. We thank Eric Salathé of the University of Washington for providing downscaled climate change scenarios for the study area. We also appreciate Joe Marek of Clackamas County, who provided valuable insights throughout the project period. Many local volunteers helped with the stream channel survey for our study sites; in particular we wish to thank Brian Wegener, Tualatin Riverkeepers, and Greg Ciannella, Johnson Creek Watershed Council, for helping to organize the volunteer effort. The article was greatly improved by the constructive comments of two anonymous reviewers.

References

- Bae, D. H., I. W. Jung, and H. Chang. 2008. Potential changes in Korean water resources estimated by high-resolution climate simulation. *Climate Research* 35:213–26.
- 595 Benito, G., A. Diez-Herrero, and M. F. de Villalta. 2003. Magnitude and frequency of flooding in the Tagus basin (Central Spain) over the last millennium. *Climatic Change* 58:171–92.
- 600 Black, W. R., and N. Sato. 2007. From global warming to sustainable transport 1989–2006. *International Journal of Sustainable Transportation* 1:73–89.
- Burlando, P., and R. Rosso. 2002. Effects of transient climate change on basin hydrology: 1. Precipitation scenarios for the Arno River, central Italy. *Hydrological Processes* 16:1151–75.
- 605 Cameron, D. 2006. An application of the UKCIP02 climate change scenarios to flood estimation by continuous simulation for a gauged catchment in the northeast of Scotland, UK (with uncertainty). *Journal of Hydrology* 328:212–26.
- 610 Carter, T. R., R. N. Jones, X. Lu, S. Bhadwal, C. Conde, L. O. Mearns, B. C. O’Neill, M. D. A. Rounsevell, and M. B. Zurek. 2007. In *Climate change 2007: Impacts, adaptation and vulnerability. Contribution of Working Group II to the Fourth Assessment Report of the Intergovernmental Panel on Climate Change*, ed. M. L. Parry, O. F. Canziani, J. P. Palutikof, P. J. van der Linden, and C. E. Hanson. Cambridge, UK: Cambridge University Press.
- Q6 620 Chang, H. 2007. Streamflow characteristics in urbanizing basins in the Portland metropolitan area, Oregon, USA. *Hydrological Processes* 21 (2): 211–22.
- Chang, H., and J. Franczyk. 2008. Climate change, land cover change, and floods: Toward integrated assessments. *Geography Compass* 2 (5): 1549–79.
- 625 Changnon, S. D. 2003. Measures of economic impacts of weather extremes. *Bulletin of the American Meteorological Society* 54:1231–35.
- Chapman, L. 2007. Transport and climate change: A review. *Journal of Transport Geography* 15:354–67. 630
- Chow, V. T. 1959. *Open-channel hydraulics*. New York: McGraw-Hill.
- Compton, K., T. Ermolieva, and J. C. Linnerooth-Bayer. 2002. Integrated flood risk management for urban infrastructure: Managing the flood risk to Vienna’s heavy rail mass rapid transit system. In *Proceedings of the Second Annual International IASA-DPRI meeting: Integrated disaster risk management: Megacity vulnerability and resilience*. Laxenburg, Austria: International Institute for Applied Systems Analysis. 635 Q7 640
- Cooper, R. M. 2005. Estimation of peak discharges for rural, unregulated streams in Western Oregon. Scientific Investigations Report 2005–5116, U.S. Geological Survey. Q8 645
- Dagnachew, L., V. C. Christine, and G. Francoise. 2003. Hydrological response of a catchment to climate and land use changes in tropical Africa: Case study south central Ethiopia. *Journal of Hydrology* 275:67–85.
- Dobney, K., C. J. Baker, A. D. Quinn, and L. Chapman. 2009. Quantifying the effects of high summer temperatures due to climate change on buckling and rail related delays in South-east United Kingdom. *Meteorological Applications* 16:254–61. 650
- Flynn, K. M., W. H. Kirby, and P. R. Hummel. 2006. User’s manual for program PeakFQ, annual flood-frequency analysis using Bulletin 17B guidelines. Techniques and Methods 4-B4, U.S. Geological Survey. 655 Q9
- Frank, M., and P. Wolfe. 1956. An algorithm for quadratic programming. *Naval Research Logistics Quarterly* 3:95–110. 660
- Gerig, A. J. 1985. *Soil survey of Clackamas County, Oregon*. U.S. Department of Agriculture, Soil Conservation Service, and Forest Service. Q10
- Gordon, C., C. Cooper, C. A. Senior, H. Banks, J. M. Gregory, T. C. Johns, J. F. B. Mitchell, and R. A. Wood. 2000. The simulation of SST, sea ice extents and ocean heat transports in a version of the Hadley Centre coupled model without flux adjustments. *Climate Dynamics* 16:147–68. 665
- Green, G. L. 1982. *Soil survey of Washington County, Oregon*. U.S. Department of Agriculture, Soil Conservation Service, and Forest Service. 670 Q11
- . 1983. *Soil survey of Multnomah County, Oregon*. U.S. Department of Agriculture, Soil Conservation Service, and Forest Service. Q12 675
- Harrelson, C. C., C. L. Rawlins, and J. P. Potyondy. 1994. Stream channel reference sites: An illustrated guide to field technique. General Technical Report RM-245, U.S. Department of Agriculture, Forest Service, Rocky Mountain Forest and Range Experiment Station. Q13 680
- Holman, I. P., M. D. A. Rounsevell, G. Cojocar, S. Shackley, C. McLachlan, E. Audsley, P. M. Berry, et al. 2008. The concepts and development of a participatory regional integrated assessment tool. *Climatic Change* 90:5–30.
- Hotchkiss, R. H., E. A. Thiele, E. J. Nelson, and P. L. Thompson. 2008. Culvert hydraulics comparison of current computer models and recommended improvements. *Transportation Research Record* 2060:141–49. 685

- Huntington, T. 2006. Evidence for intensification of the global water cycle: Review and synthesis. *Journal of Hydrology* 319:83–95.
- ICF International. 2008. The potential impacts of global sea level rise on transportation infrastructure. Fairfax, VA: ICF International. <http://www.bv.transports.gouv.qc.ca/mono/0965210.pdf> (last accessed 12 July 2009).
- Interagency Advisory Committee on Water Data. 1982. Guidelines for determining flood-flow frequency. Bulletin 17B of the Hydrology Subcommittee, Office of Water Data Coordination, U.S. Geological Survey, Reston, VA. http://water.usgs.gov/osw/bulletin17b/bulletin_17B.html (last accessed 3 June 2009).
- Intergovernmental Panel on Climate Change (IPCC). 2007. Climate change 2007: The physical science basis. Contribution of Working Group I to the Fourth Assessment Report of the Intergovernmental Panel on Climate Change. Cambridge, UK: Cambridge University Press.
- Jacob, K., V. Gornitz, and C. Rosenzweig. 2007. Vulnerability of the New York City metropolitan area to coastal hazards, including sea level rise: Inferences for urban coastal risk management and adaptation policies. In *Managing coastal vulnerability*, ed. L. McFadden, R. Nicholls, and E. Penning-Roswell, pp. 141–58. Oxford, UK: Elsevier.
- Kay, A. L., H. N. Davies, V. A. Bell, and R. G. Jones. 2009. Comparison of uncertainty sources for climate change impacts: Flood frequency in England. *Climatic Change* 92:41–63.
- Kirshen, P., K. Knee, and M. Ruth. 2008. Climate change and coastal flooding in metro Boston: Impacts and adaptation strategies. *Climatic Change* 90:453–73.
- Knight, C. G., and J. Jäger, eds. 2009. *Integrated regional assessment of global climate change*. New York: Cambridge University Press.
- Koetse, M. J., and P. Rietveld. 2009. The impact of climate change and weather on transport: An overview of empirical findings. *Transportation Research Part D-Transport and Environment* 14:205–21.
- Laenen, A., and J. C. Risley. 1997. Precipitation-runoff and streamflow routing models for the Willamette River Basin, Oregon. Water-Resources Investigation Report 95-4284, U.S. Geological Survey.
- Leavesley, G. H., S. L. Markstrom, P. J. Restrepo, and R. J. Viger. 2002. A modular approach to addressing model design, scale, and parameter estimation issues in distributed hydrological modelling. *Hydrological Processes* 16 (2): 173–87.
- Lindgreen, J., D. K. Jonsson, and A. Carlsson-Kanyama. 2009. Climate adaptation of railways: Lessons from Sweden. *EJTIR* 9 (2): 164–81.
- Lonergan, S., R. Difrancesco, and M.-K. Woo. 1993. Climate change and transportation in northern Canada: An integrated impact assessment. *Climatic Change* 24: 331–51.
- Mahmassani, H. S. 2001. Dynamic network traffic assignment and simulation methodology for advanced system management applications. *Networks and Spatial Economics* 1 (3): 267–92.
- Metro. 2009. Daily vehicle miles of travel (DVMT) for Portland. <http://www.oregonmetro.gov/index.cfm/go/by.web/id=16340> (last accessed 7 July 2009).
- National Research Council (NRC). 1999. The costs of natural disasters: A framework for assessment. Washington, DC: National Academy Press.
- . 2007. Metropolitan travel forecasting: Current practice and future direction. Transportation Research Board Special Report 288, National Academies Press, Washington, DC.
- . 2008. Transportation Research Board Special Report 290, National Academies Press, Washington, DC.
- Oregon Climate Service. 2008. Station climate data, Zone 2 <http://www.ocs.orst.edu/index.html> (last accessed 2 October 2008).
- Oregonian. 2007. Johnson Creek floods, closing nearby roads. http://blog.oregonlive.com/breakingnews/2007/12/johnson_creek_reaches_flood_st.html (last accessed 7 July 2009).
- Peeta, S., and A. K. Ziliaskopoulos. 2001. Foundations of dynamic traffic assignment: The past, the present and the future. *Networks and Spatial Economics* 1 (3): 233–65.
- Pielke, R. A., and M. W. Downton. 2000. Precipitation and damaging floods: Trends in the United States, 1932–97. *Journal of Climate* 13:3625–37.
- Randall, D. A., R. A. Wood, S. Bony, R. Colman, T. Fichefet, J. Fyfe, V. Kattsov, et al. 2007. Climate models and their evaluation. In *Climate change 2007: The physical science basis. Contribution of Working Group I to the Fourth Assessment Report of the Intergovernmental Panel on Climate Change*, ed. S. Solomon, D. Qin, M. Manning, Z. Chen, M. Marquis, K. B. Averyt, M. Tignor et al., 589–662. New York: Cambridge University Press.
- Rosenbrock, H. H. 1960. An automatic method of finding the greatest or least value of a function. *Computer Journal* 3:175–84.
- Salathé, E. P., P. W. Mote, and M. W. Wiley. 2007. Review of scenario selection and downscaling methods for the assessment of climate change impacts on hydrology in the United States Pacific Northwest. *International Journal of Climatology* 27:1611–21.
- Sohn, J. 2006. Evaluating the significance of highway network links under the flood damage: An accessibility approach. *Transportation Research Part A* 40: 491–506.
- Soleckie, W. D., and C. Rosenzweig. 2001. The impact of potential climate change in metropolitan New York. In *From the Hudson to the Hamptons: Snapshots of the New York metropolitan area*, ed. I. M. Miyares, M. Pavlovskaya, and G. Pope. Washington, DC: Association of American Geographers.
- Suarez, P., W. Anderson, V. Mahal, and T. R. Lakshmanan. 2005. Impacts of flooding and climate change on urban transportation: A systemwide performance assessment of the Boston Metro Area. *Transportation Research Part D: Transport and Environment* 10 (3): 231–44.
- Wagener, T., and H. S. Wheater. 2006. Parameter estimation and regionalization for continuous rainfall-runoff models including uncertainty. *Journal of Hydrology* 320: 132–54.
- Wilby, R. L., and I. Harris. 2006. A framework for assessing uncertainties in climate change impacts: Low-flow scenarios for the River Thames, UK. *Water Resources Research* 42:W02419.

- Wood, A. W., L. R. Leung, V. Sridhar, and D. P. Lettenmaier. 2004. Hydrologic implications of dynamic and statistical approaches to downscaling climate model outputs. *Climatic Change* 62 (1–3): 189–216.
- 815
- Wurbs, R., S. Toneatti, and J. Sherwin. 2001. Modeling uncertainty in flood studies. *International Journal of Water Resources Development* 17 (3): 353–63.

Correspondence: Department of Geography, Portland State University, 1721 SW Broadway, Portland, OR 97201, e-mail: changh@pdx.edu 820 (Chang); lafrenz@pdx.edu (Lafrenz); bobilwon@paran.com (Jung); Department of Civil and Environmental Engineering, Portland State University, 1930 SW 4th Ave, Portland, OR 97201, e-mail: figliozi@pdx.edu (Figliozi); Metro, 600 NE Grand Avenue, Portland OR 97232, e-mail: deena.platman@oregonmetro.gov (Platman); Cindy.Pederson@oregonmetro.gov (Pederson).